

Impact of Cd-Free Buffer Layer on Boosting the Performance of CIGS-Based Solar Cell

Fady Elhady¹, Walid S. Selmy², Mostafa Fedawy^{3,4}

¹Department of Basic Engineering Sciences, Benha Faculty of Engineering, Benha University, Benha, Egypt

²Department of Basic Engineering Sciences, Benha Faculty of Engineering, Benha University, Benha, Egypt

³Electronics and Communications Department, Faculty of Engineering, Arab Academy for Science and Technology and Maritime Transport, Egypt

⁴Center of Excellence in Nanotechnology, Arab Academy for Science and Technology and Maritime Transport, Egypt

Email address: ¹Fady.elhady@bhit.bu.edu.eg, ²Walid.mohamed@bhit.bu.edu.eg, ^{3,4}m.fedawy@aast.edu

Abstract— In this study, we proposed a Cd-free Cu(In,Ga)Se₂ (CIGS)-based solar cell with low-cost and high performance. This is achieved by using lead sulfide (PbS) as an electron back reflector and zinc sulfide (ZnS) as a buffer layer instead of cadmium sulfide (CdS) layer. 1D-solar cell capacitance simulator (SCAPS) was employed to optimize our proposed structure of Al-ZnO/ZnS/CIGS/PbS/Mo by investigating the effect of varying thicknesses and doping concentrations of CIGS absorber layer and ZnS buffer layer. Moreover, the effect of operating temperature on the performance of this structure was investigated. The results of the simulation of J-V characteristics showed that the efficiency of the proposed structure at 300 K is 25.5% with a 0.9 μm thickness and acceptor concentration of 10¹⁷ cm⁻³ for CIGS layer and 0.03 μm thickness and donor concentration of 3×10¹⁷ cm⁻³ ZnS layers, respectively. The proposed work improves the efficiency; in addition, the thickness of CIGS layer decreases significantly.

Keywords— Buffer; CIGS solar cell; SCAPS; ZnS.

I. INTRODUCTION

Energy is crucial for the human life. Previously, the energy was obtained from non-renewable sources such as fossil fuels and petroleum that are harmful for the environment. Hence, researchers seek to find alternative sources, which are sustainable and friendly to the environment, such as sunlight. Thus, researchers developed solar cells to harvest the light from the sun and get electricity. Solar cell manufacturing has passed through different phases, from the first generation to the next. The main goal of researchers is to find materials that achieve high performance at a low cost and in less time [1]. Compared to silicon-based solar cells, chalcopyrite-based solar cells are capable of absorbing sunlight with a small thickness without affecting their performance; as a result, the fabrication cost is reduced. Copper indium gallium (di) selenide Cu(In,Ga)Se₂ (CIGS) is a promising material that is used in chalcopyrite materials-based solar cells because it is a direct bandgap material, which can be adjusted from 1 to 1.7 eV depending on y, which the fraction of gallium in CIGS material according to equation (1) [2]. Moreover, it has a high absorption coefficient, which helps absorb the solar spectrum with a small thickness. Furthermore, CIGS is characterized by high stability and radiation resistance [3]. CIGS consists of indium and gallium elements, which are exposed to depletion; moreover, they are high-cost components [4]. Thus, scientists think that it is very

important to reduce the thickness of the CIGS as much as possible without affecting the performance significantly to keep the cost of CIGS-based solar cells low. As a result, a large number of manuscripts investigated the effect of the electron back reflector layer, which is a layer between the back contact and absorber layer, on reducing CIGS absorber layer thickness and retaining the high performance of CIGS-based solar cells [3]–[7]. On the other hand, other researchers employed the effect of the proper buffer layer to enhance the performance of CIGS solar cells [1], [8], [9].

In this study, we combine the effects of employing the electron back reflector layer (EBR) and the buffer layer. Our approach is based on the structure proposed by B. Barman *et al.* [7]; however, we replaced the CdS buffer layer with a ZnS layer to overcome the toxicity of the CdS layer [10], as shown in Fig.1. Moreover, ZnS is a promising buffer layer material because of its wider bandgap of about 3 eV compared to the CdS layer's bandgap of about 2.42 eV; thus, most of the solar spectrum can reach the absorber layer [8]. As a result, efficiency improved significantly, and CIGS thickness decreased dramatically, which leads to the decrease in the fabrication cost of these cells.

$$E_g(y) = 0.21y^2 + 0.49y + 1 \quad (1)$$

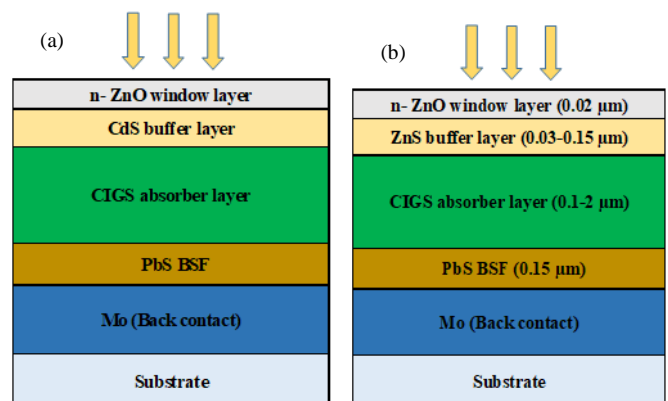


Fig.1. (a) Baseline structure of B. Barman *et al.* (b) our proposed structure of CIGS-based solar cell

II. DEVICE DESIGN AND SIMULATION

Currently, numerical modelling is crucial for investigating the physical properties of different solar cells to obtain an

optimized structure before the manufacturing stage [11]. As a result, a one-dimensional simulator called solar cell capacitance simulator (SCAPS-1D) is used in this work to optimize our proposed structure. Originally, researchers at the Department of Electronics and Information Systems (ELIS) of the University of Gent, Belgium, developed this simulator for investigating the performance of polycrystalline solar cells such as CIGS and CdTe [12]. In this simulator, up to seven layers can be added and, most parameters can be graded. Moreover, SCAPS solves the Poisson's equation together with the continuity equations to calculate the one-dimensional carrier transport, recombination profiles band diagram, and band diagram in steady state [5]. Poisson's and electron and hole continuity equations are expressed as follows, respectively:

$$\frac{d^2\psi(x)}{dx^2} = \frac{e}{\epsilon_0\epsilon_r} [p(x) - n(x) + N_D^+ - N_A^- + \rho_p - \rho_n] \quad (2)$$

$$\frac{-1}{e} \frac{dJ_n}{dx} = G(x) - R(x) \quad (3)$$

$$\frac{1}{e} \frac{dJ_p}{dx} = G(x) - R(x) \quad (4)$$

Where $\psi(x)$ is the electrostatic potential, e is electrical charge, n and p are electron and hole densities, N_D^+ is ionized donor concentration and N_A^- is ionized acceptor concentration, ρ_p and ρ_n are holes and electrons distribution, ϵ_0 is vacuum and ϵ_r is the relative permittivity, J_n and J_p are electrons and holes current densities, and G is generation rate and R recombination rate, respectively.

TABLE I. Material parameters of proposed CIGS-based solar cell.

Layers parameters	Material Parameters of Proposed CIGS-Based Solar Cell			
	p-CIGS	ZnS	n-ZnO	PbS
Layer thickness, t (μm)	0.1-2	0.03-0.15	0.02	0.15
Bandgap, E_g (eV)	1.2	3	3.3	1.2
Electron affinity, X (eV)	4.19	4.15	4.6	3.9
Relative permittivity, ϵ_r	13.6	9	9	10
Valence band effective density of states, N_v (cm^{-3})	1.8×10^{19}	1.8×10^{18}	1.8×10^{19}	2×10^{18}
Conduction band effective density of states, N_c (cm^{-3})	2.2×10^{18}	2.2×10^{18}	2.2×10^{18}	2×10^{18}
Electron thermal velocity, v_e (cm/s)	1×10^7	1×10^7	1×10^7	1×10^7
Hole thermal velocity, v_h (cm/s)	1×10^7	1×10^7	1×10^7	1×10^7
Hole mobility, μ_h (cm^2/Vs)	25	25	25	100
Electron mobility, μ_e (cm^2/Vs)	100	100	100	25
The density of acceptor, N_A (cm^{-3})	10^{16} - 10^{17}	0	0	1×10^{20}
The density of donor, N_D (cm^{-3})	0	10^{16} - 10^{18}	1×10^{20}	0
Defect concentration, N_t (cm^{-3})	1×10^{14} (D)	1×10^{17} (A)	1×10^{14} (A)	1×10^{14} (D)

Fig. 1 shows the design of our proposed CIGS-based solar cell (AZO/ ZnS/ CIGS/ PbS/ Mo). Table I and Table II

summarize the parameters of each layer used in this work [3], [7], [13]. Moreover, the absorption coefficients of CIGS and PbS are taken from [14], [15]. As shown in Fig. 1, firstly, the (Al:ZnO) window layer, which is characterized by a large bandgap to allow most of the light to reach the absorber and high conductivity for electrons to reach front contact [4]. Then, the n-ZnS buffer layer, which is a large bandgap semiconductor to let spectrum enter the absorber layer, is used to create a p-n heterojunction with p-type CIGS absorber layer [16]. Underneath the buffer layer lays the bulk layer, or called the absorber layer, which is a direct bandgap material, and its bandgap is tunable from 1 to 1.7 eV based on the gallium percent in CIGS material. After that, the PbS back surface field layer plays a crucial role in enhancing the performance of a CIGS-based solar cell by reducing the back recombination when the CIGS is small by creating an additional electric field, which reflects the electrons away from the back contact [7]. It should be a heavily doped p-type layer. On the other hand, a back contact layer such as Molybdenum (Mo), which is distinguished by high reflectivity for most of the unabsorbed photons, helps the absorber layer absorb them and form a quasi-ohmic contact with CIGS layer due to its high work function [4]. Lastly, the common substrate used in the fabrication of CIGS-based solar cells is soda lime glass.

TABLE II. Material parameters of proposed CIGS-based solar cell.

Contact Properties	Material Parameters of Proposed CIGS-Based Solar Cell	
	Front	Back (Mo)
Metalwork function Φ_m (eV)	Flat band	4.95
Surface recombination velocity of hole S_h (cm/s)	10^5	10^7
Surface recombination velocity of electron S_e (cm/s)	10^7	10^5
Reflectivity	0.05	0.90

III. RESULTS AND DISCUSSION

The use of large bandgap buffer layer is an effective approach to enhance the performance of the CIGS-based solar cell. Our proposed structure (Al-ZnO/ZnS/CIGS/PbS/Mo) is based on the cell proposed by B. Barman et al. (2021). In this work, the illumination of AM1.5 with an incident power of 1000 W/m², and a temperature of 300 K are used for all simulations.

A. Effect of varying CIGS thickness

In this stage, CIGS thickness varies from 0.1 to 2 μm ; however, other parameters are the same as in Table I. As shown in Fig. 2.a, J_{SC} increases with the increase in the CIGS thickness because of the increase in the number of photons absorbed in this layer [17]. However, V_{OC} decreases as the CIGS thickness increases due to the increase in the probability of recombination. As depicted in Fig.2.b, FF and efficiency increase significantly when the thickness of CIGS increases until CIGS thickness of 0.9 μm . After this thickness, FF appears constant; however, efficiency decreases slightly. The improvement in the power conversion efficiency is due to the significant increase in J_{SC} and FF. As a result, the optimum thickness of CIGS layer is 0.9 μm , which gives the efficiency of 23.33%.

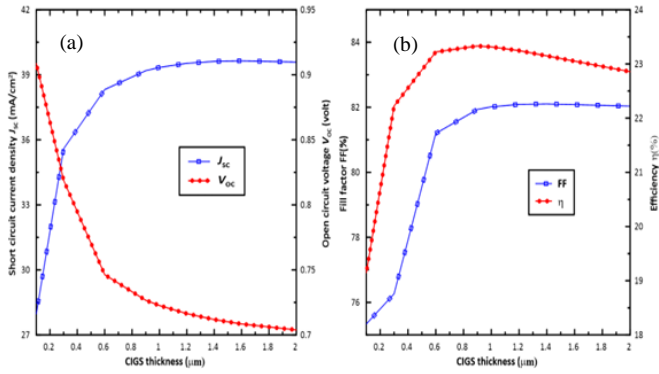


Fig. 2. Effect of CIGS thickness on (a) J_{sc} and V_{oc} (b) FF and Efficiency

B. Effect of varying ZnS thickness

Here, ZnS thickness is changed from 0.03 to 0.15 μm ; however, other parameters of the layers are still the same except CIGS thickness is set to 0.9 μm . J_{sc} decays with the rise in thickness of ZnS buffer layer because part of the light is absorbed in this layer; hence the number of photons absorbed by the absorber layer decreases [18]; in addition, V_{oc} can be considered almost constant as shown in Fig.3.a. Furthermore, efficiency decreases slightly with the increase in the thickness of ZnS; however, FF increases more slightly, as depicted in Fig. 3.b. As a result, the optimum value of buffer layer thickness is 0.03 μm with efficiency of 23.33%.

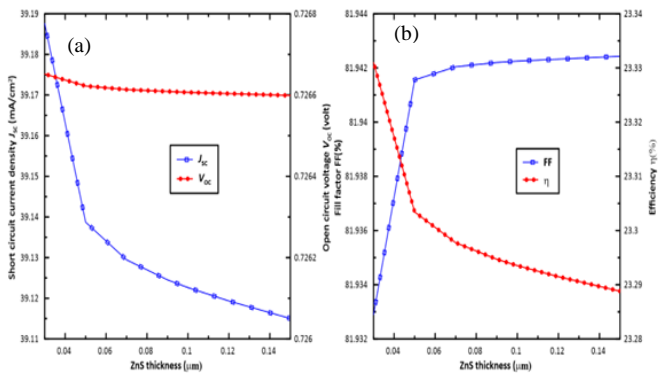


Fig. 3. Effect of ZnS thickness on (a) J_{sc} and V_{oc} (b) FF and Efficiency

C. Effect of CIGS acceptor concentration

Fig. 4 shows the effect of CIGS acceptor concentration N_A , which is changed from $1 \times 10^{16} \text{ cm}^{-3}$ to $1 \times 10^{17} \text{ cm}^{-3}$ on the solar cell parameters. As shown in Fig.4.a, as CIGS acceptor concentration increases, J_{sc} decreases slightly due to the increase in recombination in the bulk of the absorber layer [8]; however, V_{oc} increases. Moreover, FF and efficiency increase when N_A increases due to improvement in open circuit voltage, as presented in Fig.4.b. As a result, the optimum value of N_A is 10^{17} cm^{-3} and the efficiency is 25.06%.

D. Effect of ZnS donor concentration

Fig.5 shows the effect of ZnS acceptor concentration N_D on the solar cell parameters. Donor concentration varies from $1 \times 10^{16} \text{ cm}^{-3}$ to $1 \times 10^{18} \text{ cm}^{-3}$. As shown in Fig.5.a, when ZnS donor concentration increases, J_{sc} increases until the value of $7 \times 10^{17} \text{ cm}^{-3}$, then it decreases; however, V_{oc} decreases slightly. On the other hand, FF and efficiency increase when N_A

increases until the value of $3 \times 10^{17} \text{ cm}^{-3}$, then they decrease slightly, as presented in Fig.4.b. Thus, the optimum value of N_D is $3 \times 10^{17} \text{ cm}^{-3}$ the power conversion efficiency is 25.5%.

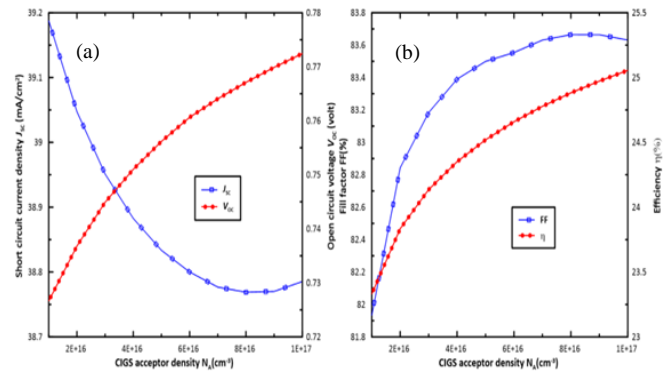


Fig. 4. Effect of CIGS acceptor concentration on (a) J_{sc} and V_{oc} (b) FF and Efficiency

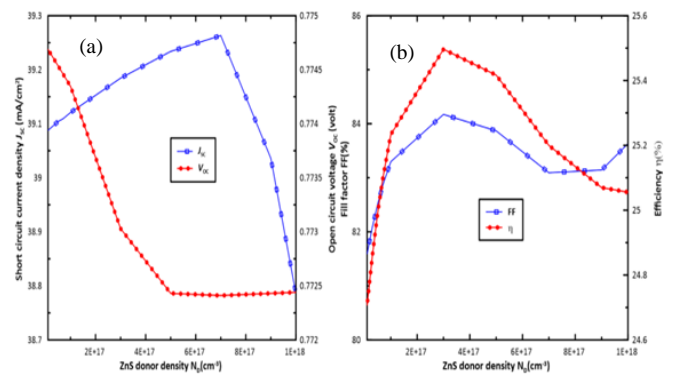


Fig. 5. Effect of ZnS donor concentration on (a) J_{sc} and V_{oc} (b) FF and Efficiency

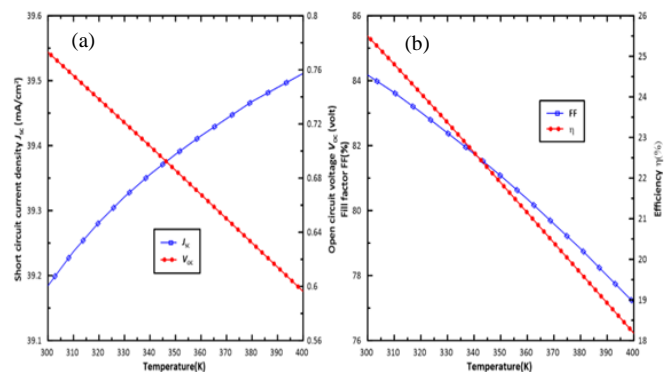


Fig. 6. Effect of operating temperature on (a) J_{sc} and V_{oc} (b) FF and Efficiency

E. Effect of operating temperature

Here, the impact of the operating temperature, which is varied from 300 K to 400 K is investigated on the solar cell performance. As shown in Fig.6.a, V_{oc} decreases significantly with the increase in operating temperature because of increase in the reverse saturation current (i.e., recombination rate increases). However, J_{sc} increases slightly with the increase in temperature due to the increase of electron-hole pairs generated thermally due to the decrease in the energy bandgap [19]. On the other hand, FF and efficiency decrease significantly when

operating temperature increases as shown in Fig.6.b. Consequently, the best value of temperature is 300 K, which gives the best performance with the efficiency of 25.5%.

ACKNOWLEDGMENT

The authors thankfully acknowledge SCAPS-1D simulator originators at the Electronics and Information Systems (ELIS) department at the University of Gent, Belgium.

The authors also gratefully acknowledge the center of excellence in nanotechnology, Arab Academy for Science and Technology and Maritime Transport (AASTMT), Cairo, Egypt.

REFERENCES

- [1] Z. R. Abdulghani, A. S. Najm, A. M. Holi, A. A. Al-Zahrani, K. S. Al-Zahrani, and H. Moria, "Numerical simulation of quantum dots as a buffer layer in CIGS solar cells: A comparative study," *Sci. Rep.*, vol. 12, no. 1, pp. 1–16, 2022.
- [2] F. Elhady, T. M. Abdolkader, and M. Fedawy, "Simulation of new thin film Zn (O, S)/CIGS solar cell with bandgap grading," *Eng. Res. Express*, vol. 5, no. 2, p. 25027, 2023.
- [3] H. Heriche, Z. Rouabah, and N. Bouarissa, "New ultra thin CIGS structure solar cells using SCAPS simulation program," *Int. J. Hydrogen Energy*, vol. 42, no. 15, pp. 9524–9532, 2017, doi: 10.1016/j.ijhydene.2017.02.099.
- [4] Y. Osman, M. Fedawy, M. Abaza, and M. H. Aly, "Optimized CIGS based solar cell towards an efficient solar cell: impact of layers thickness and doping," *Opt. Quantum Electron.*, vol. 53, no. 5, p. 245, 2021, doi: 10.1007/s11082-021-02873-4.
- [5] T. Alzoubi and M. Moustafa, "Simulation analysis of functional MoSe₂ layer for ultra-thin Cu (In, Ga) Se₂ solar cells architecture," *Mod. Phys. Lett. B*, vol. 34, no. 05, p. 2050065, 2020.
- [6] S. R. I. Biplab, M. H. Ali, M. M. A. Moon, M. F. Pervez, M. F. Rahman, and J. Hossain, "Performance enhancement of CIGS-based solar cells by incorporating an ultrathin BaSi₂ BSF layer," *J. Comput. Electron.*, vol. 19, no. 1, pp. 342–352, Mar. 2020, doi: 10.1007/s10825-019-01433-0.
- [7] B. Barman and P. K. Kalita, "Influence of back surface field layer on enhancing the efficiency of CIGS solar cell," *Sol. Energy*, vol. 216, pp. 329–337, 2021.
- [8] A. Bensaad, A. Garadi, A. Beloufa, and Z. Bensaad, "Efficiency enhancement of Cd-free buffer layers on CIGS solar cell performance using WxAMPS," *Optik (Stuttg.)*, vol. 267, p. 169736, 2022.
- [9] T. J. Mebelson and K. Elampari, "Numerical simulation for optimal thickness combination of CdS/ZnS dual buffer layer CuInGaSe₂ solar cell using SCAPS 1D," *Indian J. Sci. Technol.*, vol. 12, no. 45, pp. 1–6, 2019.
- [10] H. I. Abdalmageed, M. Fedawy, and M. H. Aly, "Effect of absorber layer bandgap of CIGS-based solar cell with (CdS/ZnS) buffer layer," in *Journal of Physics: Conference Series*, 2021, vol. 2128, no. 1, p. 12009.
- [11] A. Morales-Acevedo, N. Hernández-Como, and G. Casados-Cruz, "Modeling solar cells: a method for improving their efficiency," *Mater. Sci. Eng. B*, vol. 177, no. 16, pp. 1430–1435, 2012.
- [12] M. Burgelman, P. Nollet, and S. Degraeve, "Modelling polycrystalline semiconductor solar cells," *Thin Solid Films*, vol. 361, pp. 527–532, 2000.
- [13] M. Boubakeur *et al.*, "Enhancement of the efficiency of ultra-thin CIGS/Si structure for solar cell applications," *Superlattices Microstruct.*, vol. 138, no. December 2019, p. 106377, 2020, doi: 10.1016/j.spmi.2019.106377.
- [14] K. Kim *et al.*, "Performance prediction of chalcopyrite-based dual-junction tandem solar cells," *Sol. Energy*, vol. 155, pp. 167–177, 2017, doi: <https://doi.org/10.1016/j.solener.2017.05.080>.
- [15] K. Aadim, A. Ibrahim, and J. Marie, "Structural and optical properties of PbS thin films deposited by pulsed laser deposited (PLD) technique at different annealing temperature," *Int. J. Phys.*, vol. 5, no. 1, pp. 1–8, 2017.
- [16] M. S. R. Robin, M. M. M. Rasmi, M. S. Z. Sarker, and A. S. M. R. Al Mamun, "Numerical modeling and analysis of ultra thin film Cu(In, Ga)Se₂ solar cell using SCAPS-1D," in *2016 3rd International Conference on Electrical Engineering and Information Communication Technology (ICEEICT)*, 2016, pp. 1–5, doi: 10.1109/ICEEICT.2016.7873169.
- [17] M. Al-Hattab, M. Khenfouch, O. Bajjou, Y. Chrafih, and K. Rahmani, "Numerical simulation of a new heterostructure CIGS/GaSe solar cell system using SCAPS-1D software," *Sol. energy*, vol. 227, pp. 13–22, 2021.
- [18] N. Khoshsirat and N. A. M. Yunus, "Numerical simulation of CIGS thin film solar cells using SCAPS-1D," in *2013 IEEE Conference on Sustainable Utilization and Development in Engineering and Technology (CSUDET)*, 2013, pp. 63–67, doi: 10.1109/CSUDET.2013.6670987.
- [19] H. Heriche, Z. Rouabah, and N. Bouarissa, "New ultra thin CIGS structure solar cells using SCAPS simulation program," *Int. J. Hydrogen Energy*, vol. 42, no. 15, pp. 9524–9532, 2017, doi: 10.1016/j.ijhydene.2017.02.099.